Physics Letters B 738 (2014) 268–273

Contents lists available at ScienceDirect

Physics Letters B

www.elsevier.com/locate/physletb

Measurement of polarisation observables in $K^0_S\Sigma^+$ photoproduction off the proton

R. Ewald [a,1], A.V. Anisovich [b,c], B. Bantes [a], O. Bartholomy [b], D. Bayadilov [b,c], R. Beck [b], Y.A. Beloglazov [c], K.-T. Brinkmann [f], V. Crede [e], H. Dutz [a], D. Elsner [a], K. Fornet-Ponse [a], F. Frommberger [a], Ch. Funke [b], A.B. Gridnev [c], E. Gutz [f], J. Hannappel [a], W. Hillert [a], P. Hoffmeister [b], I. Jaegle [d], O. Jahn [a], T.C. Jude [a,*], J. Junkersfeld [b], H. Kalinowsky [b], S. Kammer [a], V. Kleber [a,2], Frank Klein [a], Friedrich Klein [a], E. Klempt [b], B. Krusche [d], M. Lang [b], H. Löhner [g], I.V. Lopatin [c], D. Menze [a], T. Mertens [f], J.G. Messchendorp [g], V. Metag [f], M. Nanova [f], V.A. Nikonov [b,c], D. Novinski [b,c], R. Novotny [f], M. Ostrick [a,3], L. Pant [g,4], H. van Pee [b], A. Roy [g,5], A.V. Sarantsev [b,c], S. Schadmand [g,6], C. Schmidt [b], H. Schmieden [a], B. Schoch [a], S. Shende [g], V. Sokhoyan [b], A. Süle [a], V.V. Sumachev [c], T. Szczepanek [b], U. Thoma [b], D. Trnka [f], R. Varma [g], D. Walther [b], Ch. Wendel [b]

[a] Physikalisches Institut, Universität Bonn, Germany
[b] Helmholtz Institut für Strahlen- und Kernphysik, Universität Bonn, Germany
[c] Petersburg Nuclear Physics Institute, Gatchina, Russia
[d] Departement Physik, Universität Basel, Switzerland
[e] Department of Physics, Florida State University, Tallahassee, USA
[f] II. Physikalisches Institut, Universität Gießen, Germany
[g] Kernfysisch Versneller Instituut, Groningen, The Netherlands

ARTICLE INFO

Article history:
Received 16 June 2014
Received in revised form 18 September 2014
Accepted 18 September 2014
Available online 26 September 2014
Editor: D.F. Geesaman

Keywords:
Meson production
Other strange mesons
Baryon resonances (S=C=B=0)
Decays of baryons
Polarisation in interactions and scattering

ABSTRACT

The reaction $\gamma p \to K^0_S\Sigma^+$ is studied in the photon energy range from threshold. Linearly polarised photon beams from coherent bremsstrahlung enabled the first measurement of photon beam asymmetries in this reaction up to $E_\gamma = 1650$ MeV. In addition, the recoil hyperon polarisation was determined through the asymmetry in the weak decay $\Sigma^+ \to p\pi^0$ up to $E_\gamma = 2250$ MeV. The data are compared to partial wave analyses, and the possible impact on the interpretation of a recently observed prominent structure in the cross section near the K^* thresholds is discussed.

1. Introduction

The CBELSA/TAPS experiment at the Electron Stretcher Accelerator ELSA is devoted to the investigation of the structure of the nucleon at low energies. While the high energy and associated short distance dynamics are well understood and put into the commonly accepted frame of quantum chromodynamics (QCD), our knowledge is still rather limited at the size/mass scale of the nucleon. The study of excitations is hoped to provide a clue to the intra-nucleon/baryon interactions, in particular the degrees of freedom

* Corresponding author.
E-mail address: jude@physik.uni-bonn.de (T.C. Jude).
[1] Now at DLR, Cologne, Germany.
[2] Now at German Research School for Simulation Sciences, Jülich, Germany.
[3] Now at Institut für Kernphysik, Universität Mainz, Germany.
[4] On leave from Nucl. Phys. Division, BARC, Mumbai, India.
[5] On leave from Department of Physics, IIT, Mumbai, India.
[6] Present address: Institut für Kernphysik and Jülich Center for Hadron Physics, Forschungszentrum Jülich, Germany.

http://dx.doi.org/10.1016/j.physletb.2014.09.039

effective at work. These are not necessarily just quarks and gluons mediating the colour force between them. Due to the closeness of the chiral symmetry breaking scale to the nucleon mass/size scale, the associated Goldstone bosons also enter as effective "elementary" objects [1,2]. It therefore does not come as a surprise that in some aspects, models which include interactions of the light mesons with quarks are more successful than genuine three quark models with pure colour interactions in for example, the parity ordering of the lowest nucleon excitations [1]. Meson–baryon interactions appear to play an important role in baryon excitations [3–11]. Some of the states which persistently resisted a conventional three-quark explanation, for example the $N^*(1440)1/2^+$ "Roper resonance" or the $\Lambda(1405)$, are likely "dynamically" generated through meson–baryon interactions at least to some extent. In addition to the interaction of pseudoscalar mesons with baryons, vector mesons should also contribute to dynamic resonance formation [12–14]. Degenerate states of $J^P = 1/2^-, 3/2^-$ are then expected, in particular in the mass region around 2 GeV [15].

Recently, such states may have been found in the photoproduction reaction $\gamma + p \to K^0_S \Sigma^+$ [16,17]. A rapid fall of the cross section with increasing energy is observed in the vicinity of the $K^*\Lambda/\Sigma^0$ thresholds, changing from forward peaked to a flat angular distribution. The effect is strong enough to generate a prominent structure in the total cross section. In Ref. [16] this is discussed as the possible changeover from a t-channel mechanism in K^0 photoproduction to the formation of an intermediate s-channel with $L = 0$ internal angular momentum formed by a K^* vector meson interacting with an intermediate Λ or Σ hyperon.

In order to further investigate the reaction mechanism between K^0 and K^* thresholds, the analysis of the data reported in Ref. [16] was extended. In addition to the unpolarised cross sections, the photon beam asymmetry and the hyperon recoil polarisation were also extracted [18]. This paper is organised as follows: The next section gives a brief description of the experiment. Sections 3 and 4 describe the extraction of beam asymmetry and recoil polarisation. The results are then discussed in Section 5, and the paper concludes with a summary and outlook.

2. Experiment

Using the combined Crystal Barrel [19] and TAPS [20,21] detector system, the experiment was carried out at the Electron Stretcher Accelerator ELSA [22] of the University of Bonn's Physikalisches Institut. At an electron beam energy of $E_0 = 3.2$ GeV, tagged photon beams were generated by coherent bremsstrahlung from a 500 µm thick diamond radiator. Linear polarisation is obtained within the coherent intensity peaks. The plane of linear polarisation and the energy of the coherent peaks were both chosen through the orientation of the radiator crystal relative to the electron beam by means of a commercial goniometer. The coherent peaks were set at photon energies of $E_\gamma = 1305, 1515,$ and 1610 MeV, with maximum photon polarisations of $P_\gamma = 0.49, 0.42,$ and 0.39 respectively. The method of coherent bremsstrahlung and the performance of the setup are described in detail in Ref. [23].

The bremsstrahlung electrons were momentum analysed in a magnetic "tagging" spectrometer, using a 480 channel scintillating fibre detector at high electron energies (corresponding to low photon energies, i.e. high rates), and a MWPC at low electron energies, i.e. low rates. A photon energy range of $E_\gamma = 0.18$–$0.92 E_0$ was covered with an energy resolution between 10 and 25 MeV, depending on the energy of the tagging electron. Accurate tagger timing information was provided by 14 slightly overlapping scintillator bars. The tagging system was run at electron rates up to 10^7 Hz. The absolute photon flux was measured [16], but practically cancelled out in the polarisation observables presented here.

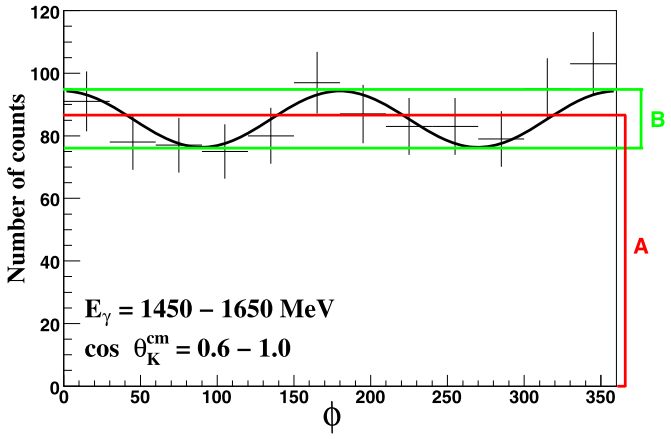

Fig. 1. Example of the azimuthal modulation of the K^0 yield in one bin (interval inset). From a fit of the function $f(\phi) = A(1 - \frac{B}{A}\cos 2\phi)$ the product $P_{lin}\Sigma_\gamma$ is determined as described in the text.

The photon beam impinged upon a liquid hydrogen target contained in a 5.3 cm long cell with 80 µm Kapton windows. The reaction products were observed in the Crystal Barrel and TAPS spectrometers, augmented by a cylindrical three layer scintillating fibre detector [24] inside the barrel. In total, the detector system covered a polar angular range of 5.8–165 degrees. Further details of setup and readout are given, for example, in Refs. [25,26].

The detector setup is ideally suited for multi-photonic final states. Therefore, the $K^0\Sigma^+$ reaction was investigated in the neutral decay modes $K^0_s \to \pi^0\pi^0$ (B.R. 31.4%) and $\Sigma^+ \to p\pi^0$ (B.R. 51.6%), yielding 6 photons and the proton. Event selection and data analysis were done as described in [16]. Here we concentrate on the aspects which are important to extract the polarisation observables.

3. Photon beam asymmetry

Accounting for a linearly polarised photon beam, the cross section of photoproduction of pseudoscalar mesons off a nucleon can be written in the form [27]

$$\frac{d\sigma}{d\Omega} = \left(\frac{d\sigma}{d\Omega}\right)_0 (1 - P_{lin}\Sigma_\gamma \cos 2\phi), \tag{1}$$

where $(d\sigma/d\Omega)_0$ is the polarisation independent cross section, P_{lin} the degree of linear polarisation, and Σ_γ the photon beam asymmetry. The product $P_{lin}\Sigma_\gamma$ determines the magnitude of modulation of the cross section with the azimuthal angle ϕ between the plane of linear polarisation and the ejected meson. This ϕ-angular modulation was determined as described in Ref. [26] by separate fits of the function

$$f(\phi) = A\left(1 - \frac{B}{A}\cos(2\phi)\right) \tag{2}$$

to the K^0 yield in three bins of photon energy (1050–1250, 1250–1450, and 1450–1650 MeV) and five bins in the centre-of-mass polar angle of the K^0 (θ_K^{cm}), each 0.4-wide in $\cos\theta_K^{cm}$. An example is shown in Fig. 1. The beam asymmetry, Σ_γ, can be extracted once the degree of beam polarisation is determined from the form of the tagged electron spectrum as also described in Ref. [26].

While unpolarised background leaves the absolute amplitude of the azimuthal modulations unchanged, it affects the relative

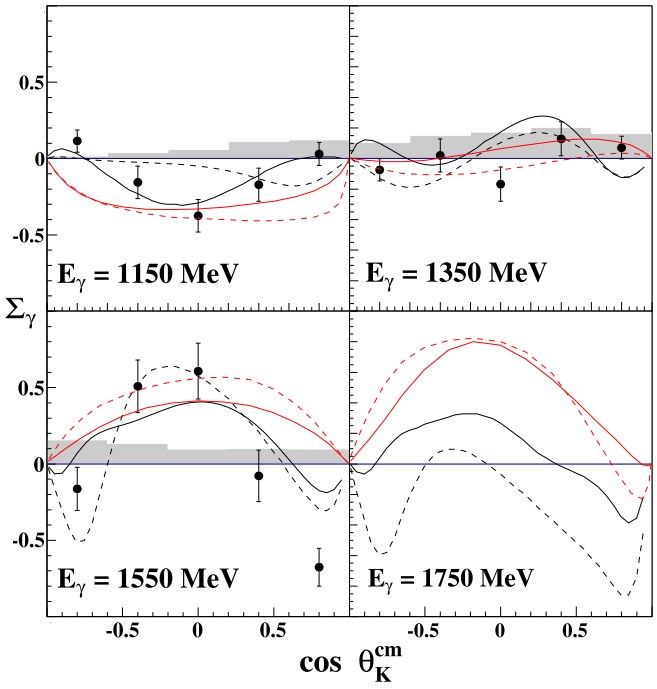

Fig. 2. Angular distribution of the photon beam asymmetry Σ_γ in the three bins of photon energy indicated in the diagrams. The error bars attached to the data points are purely statistical, the systematic errors are indicated by the grey bars on the abscissa. Curves represent the results of the Bonn–Gatchina-PWA [29] solutions, BG2011-02m (black dashed) and BG2011-02 (black solid), and the K-MAID [30] parametrisations, standard (red solid) and modified as in Ref. [16] to study the origin of the cross section anomaly at the K^* threshold (red dashed). The fourth energy bin is added to show the behaviour of the parametrisations across the K^* thresholds where there are no data yet available. (For interpretation of the references to colour in this figure legend, the reader is referred to the web version of this article.)

strength through the denominator of B/A in Eq. (2). Hence, background subtraction in the azimuthal yield spectra is as important as for cross section measurements and was performed as in [16]. Polarised background would even modify the angular modulation. Therefore, the dominating background channel of $2\pi^0$ production was investigated in this respect. It did not show any azimuthal asymmetries for invariant masses close to the K^0 mass distribution, so no correction of the absolute magnitude of the observed modulation was necessary.

The extracted azimuthal asymmetries are generally susceptible to detector (and/or analysis) inefficiencies which vary with ϕ. Such instrumental effects were extensively studied in Refs. [26,28] and were investigated in the same way for the $K^0\Sigma^+$ channel: A pure $\cos 2\phi$ distribution as is expected from the reaction cross section carries redundant information in the two intervals $\phi = [0, \pi]$ and $[\pi, 2\pi]$. Therefore fitted individually, both intervals are expected to yield the same result for the fit parameters A and B of Eq. (2). Deviations are taken as contributions to the systematic error. To avoid large statistical fluctuations in these deviations, the systematic error contribution is averaged over each energy bin with the adjacent bins and weighted according to the statistical error. Uncertainties in background subtraction were found to be less important and uncertainties in the beam polarisation were determined as 2% [23], which was considered negligible to the extracted asymmetries.

The results for the beam asymmetries are shown in Fig. 2. Attached to the data points are the statistical errors. The grey bars on the abscissa indicate the systematic errors which are obtained by adding the individual contributions in quadrature.

The curves in Fig. 2 show parametrisations of $\gamma p \to K^0_S\Sigma^+$ photoproduction. The Bonn–Gatchina PWA [29] and K-MAID [30] are both represented in two versions: The Bonn–Gatchina solution BG2011-02 (black solid) includes $\gamma p \to K^0_S\Sigma^+$ recoil polarisation data of previous CBELSA/TAPS measurements [31], however no photon asymmetry data. BG2011-02m (black dashed, see Ref. [25] for a detailed description) is an improved variant of the Bonn–Gatchina solution BG2011-02, including our beam asymmetry data in Fig. 2 and new CLAS $\gamma p \to K^0_S\Sigma^+$ recoil polarisation data [32]. K-MAID with standard parameters is shown as the solid red line, and with 'modified' parameters in red. The modification is discussed in Ref. [16]. Essentially, the K^* t-channel exchange was switched off to study the effect on the cross section in the region of the cusp-like anomaly at the K^* threshold, cf. [16]. A (re-) fit of the data was not attempted with K-MAID, neither in the standard nor the modified version.

Our measurement is the first one yet of the photon beam asymmetry in this reaction channel. Therefore, no comparison to other data can be made in Fig. 2. The data show interesting behaviour. At threshold the photon beam asymmetry is negative,[7] then compatible with zero throughout the intermediate energy bin. At higher energies the beam asymmetry changes sign and turns clearly positive, except at forward directions where it becomes strongly negative. The highest energy bin shown in Fig. 2 illustrates the behaviour of the parameterisations across the K^* thresholds, which are at $E_\gamma = 1678.2$ MeV ($E_{cm} = 2007.4$ MeV) for the $K^{*+}\Lambda$ final state, and at $E_\gamma = 1848.1$ MeV ($E_{cm} = 2085.5$ MeV) for $K^{*0}\Sigma^+$. Unfortunately, there are no data yet. The same data of Fig. 2 are presented in dependence of the photon beam energy, E_γ, in Fig. 3.

4. Recoil polarisation

In meson photoproduction the recoiling baryons generally carry polarisation. With linearly polarised photon beams, $\sin 2\varphi$ and $\cos 2\varphi$ modulations of the recoil polarisation are obtained [33]. The angle φ denotes the azimuth between the plane of linear polarisation and the reaction plane which is spanned by the ejected kaons and hyperons. Due to the lack of statistics however, in the present analysis all relative orientations of polarisation and reaction planes were integrated over. This, effectively, corresponds to unpolarised photons, in which case only one polarisation component remains non-zero. This is usually called the recoil polarisation, $\vec{P}$, and due to parity conservation it is oriented normal to the reaction plane.

In the studied reaction, the weak decay of the final state Σ^+ enables the reconstruction of the magnitude of its recoil polarisation, P. The decay angular distribution has the form

$$W(\theta_p) = \frac{1}{2}(1 + \alpha_0 P \cos\theta_p) \tag{3}$$

with α_0 denoting the so-called decay parameter, and θ_p the angle between the decay proton direction and the normal of the reaction plane. Consequently, a count rate asymmetry

$$\frac{N_\uparrow - N_\downarrow}{N_\uparrow + N_\downarrow} = \frac{1}{2}\alpha_0 P \tag{4}$$

is obtained relative to the reaction plane, where $N_\uparrow$ and $N_\downarrow$ represent the event numbers above and below, respectively. A particular benefit of the $\Sigma^+ \to \pi^0 p$ decay observed in our experiment is the large decay parameter $\alpha_0 = -0.980$ [34]. According to Eq. (4) it results in large asymmetries from which the recoil polarisation was then determined.

[7] Note that it is bounded to zero at $|\cos\theta| = 1$.

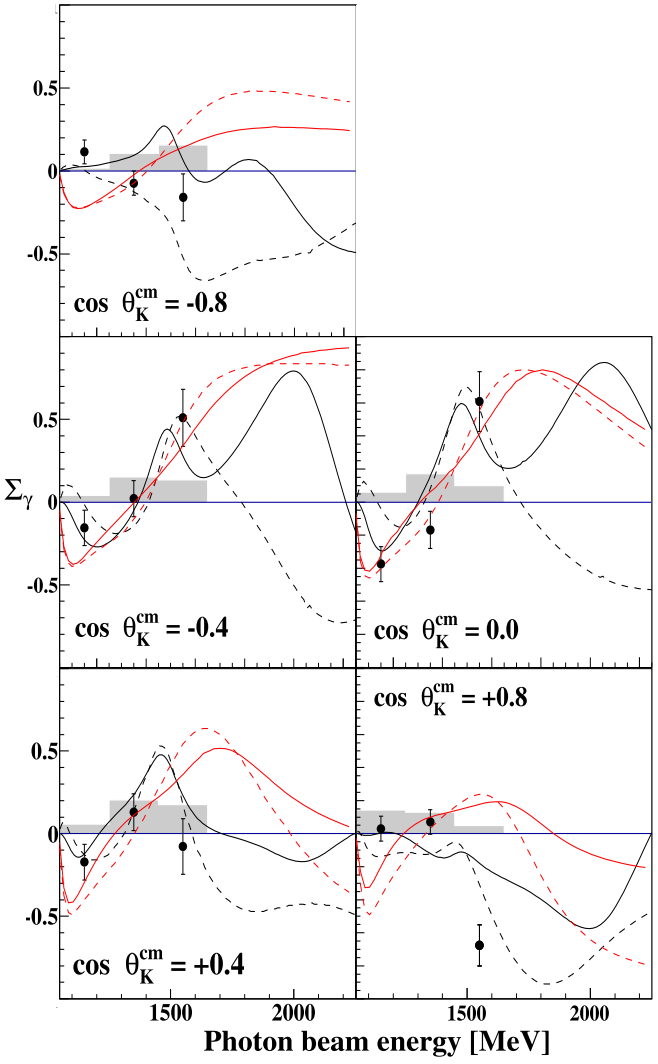

Fig. 3. Energy dependence of the photon beam asymmetry, Σ_γ, in the measured five bins of $\cos\theta_K^{cm}$. Errors and curves are as in Fig. 2. (For interpretation of the references to colour in this figure legend, the reader is referred to the web version of this article.)

In Fig. 4 our results are compared to previous measurements of the CBELSA/TAPS Collaboration, where a similar detector setup but unpolarised beam was used [31], and of SAPHIR [35]. The errors attached to the data points are purely statistical, the shaded bands on the abscissa give an estimate of the systematic uncertainties. Since, according to Eq. (4), the recoil polarisation is determined from a ratio of event rates, some of the systematic effects cancel out which may affect cross section or beam asymmetry measurements. Among those are photon flux, detector inefficiencies and beam polarisation. Remaining systematic errors were studied by variations of the cuts applied in the analysis as described in Ref. [16].

The SAPHIR data shown in Fig. 4 have different binning from our experiment, as stated in the figure. The SAPHIR results are compared in the bins where the weighted mean energy is closest. The previous measurements of the CBELSA/TAPS Collaboration binned the data into finer intervals. The data shown in Fig. 4 have the same mean energies as this new data and the energy intervals are given in the figure. In general the data sets agree fairly well, with the older CBELSA/TAPS data appearing slightly low in comparison, but still within errors. The errors of the present measurement

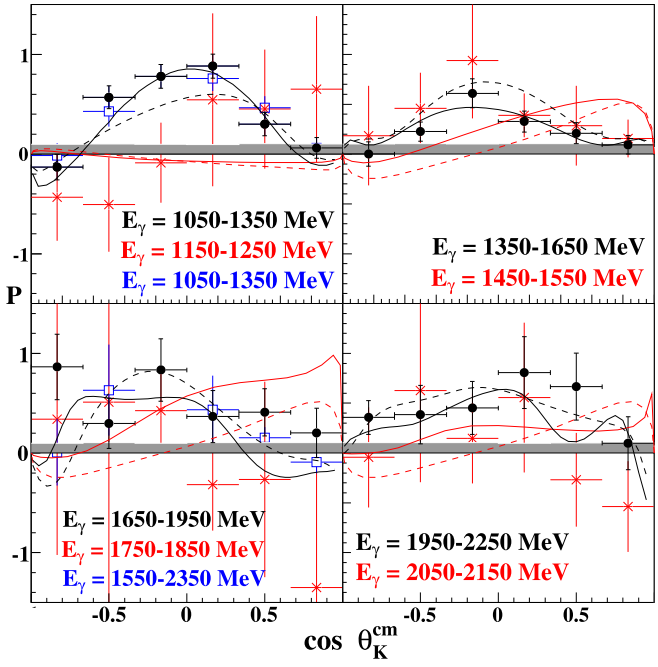

Fig. 4. Recoil polarisation of the Σ^+ in the four bins of photon energy indicated in the diagrams. The results of the present measurement (black dots) are compared to the previous CBELSA/TAPS (red crosses) [31] and SAPHIR [35] (blue squares) data. The latter data sets have different binning as indicated. Vertical bars represent the statistical errors, the horizontal lines attached to our data points are the bin widths in $\cos\theta_K^{cm}$. The systematic errors are indicated by the grey bars on the abscissa. Curves are the same as in Fig. 2. (For interpretation of the references to colour in this figure legend, the reader is referred to the web version of this article.)

represent a significant improvement, in particular at lower energies. In some energy regions this is also partly due to the use of coherent bremsstrahlung. Even though the beam polarisation was integrated over, the coherent peaks still yielded a differential increase of photon flux.

5. Discussion

The photon beam asymmetry and recoil polarisation are both observables indispensable to extract the reaction amplitudes [36], and hence the partial wave amplitudes, in a reliable manner. The curves in Figs. 2–4 demonstrate the level of agreement with the present polarisation data which can be obtained by K-MAID [30] and the Bonn–Gatchina coupled channels PWA [29].

Throughout the measured kinematic range neither version of K-MAID reproduces the recoil polarisation data. There is better agreement with the PWA solution BG2011-02m in particular, which, in contrast to K-MAID, used the present data of recoil polarisation and beam asymmetry as input for the fits. Through interferences, the recoil polarisation is very sensitive to even small partial wave contributions. Hence, the observed discrepancies point to a yet incomplete resonance basis in K-MAID.

The general features of the new beam asymmetry data are reasonably described by the different parameterisations. Both the $K^0\Sigma^+$ recoil polarisation and beam asymmetry data are important inputs for the Bonn–Gatchina PWA. The BG2011-02 solution previously found a large contribution from a $J^P = 3/2^+$ partial wave and almost negligible contribution from $J^P = 3/2^-$. The inclusion of the new data however requires a significant $J^P = 3/2^-$ contribution over a large energy range. Two very similar solutions were found, almost within statistical error: In the first solution, a larger contribution from $J^P = 3/2^-$ than $J^P = 3/2^+$ describes the asymmetry data better than the recoil asymmetry data. The opposite

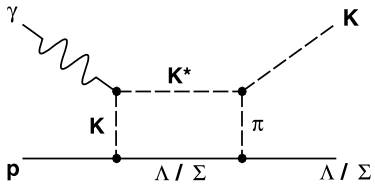

Fig. 5. t-exchange diagram for K^0 photoproduction, with an intermediate K^0 and pion rescattering through subthreshold K^* decay.

was true for the second solution. The pole structure, which is also defined by the differential cross section, remains nearly stable in both solutions.

At a mass of approximately 1880 MeV, the PWA indicates a doublet of negative parity $J^P = 1/2^-$ and $3/2^-$ states [37], as expected by chiral symmetry restoration in high mass states [38]. These two nucleon resonances can be interpreted as partners of the $J^P = 1/2^+$ and $3/2^+$ positive parity doublet at nearly the same mass or, alternatively, as members of the SU(6) 56-plet expected in the third excitation band of the nucleon [37,39]. At higher energies in the regime of the K^* thresholds the $3/2^-$ partial wave still appear significant. This is also expected for the reaction mechanism hypothesised in Ref. [16], where the intermediate K^* and Λ or Σ couple in an S-wave (Fig. 5) to form a quasi-bound state.

While the parametrisations of the photon beam asymmetry agree reasonably well with the new data at intermediate angles, the highest energy data in the forward bins in particular, appear more negative than expected (Fig. 3 bottom right and Fig. 2 bottom left). The statistical accuracy of the data and steep energy dependence of the parameterisations at these angles preclude any definite conclusions, however, this is an interesting region for further investigation as it is just below the prominent structure observed in the forward cross section [16].

Close to the K^* threshold, quasibound K^*-hyperon states are expected in chiral unitary approaches through the interaction of the nonet of vector mesons with the octet of baryons [14]. If a quasi-bound vector meson–hyperon state was formed, the beam asymmetry would be expected to show structures which are sensitive to this. No model calculations have yet investigated the effect on the beam asymmetry in detail. However, there are recent calculations [17] to study the observed cross section anomaly in $K^0\Sigma^+$ photoproduction [16]. Subthreshold K^* production and subsequent rescattering may be responsible for the strong downturn of the $K^0\Sigma^+$ cross section at the K^* thresholds. The effect appears associated with a delicate interference between $K^*\Lambda$ and $K^*\Sigma$ intermediate states which is found strongly destructive off the proton, but much less off the neutron. This offers a way to test the model. Our new data, in particular the photon asymmetry, provide a further testing ground for such models.

It is desirable to further extend the data base. The energy range of the presented beam asymmetry data is still restricted to somewhat below the K^* thresholds. To shed more light on the reaction mechanism and the possible formation of a dynamically generated vector meson–baryon state, it will be mandatory to extend measurements over and beyond the K^* thresholds, where the PWA solutions have the largest discrepancies.

6. Summary and outlook

Single polarisation observables in $K^0\Sigma^+$ photoproduction off the proton were measured. The recoil polarisation, P, was determined from threshold to $E_\gamma = 2250$ MeV, agreeing well with previous measurements. While the description by the K-MAID parametrisation without attempting to fit the new data remains unsatisfactory, new fits bring the Bonn–Gatchina PWA into good agreement with the measured recoil polarisations [37].

The photon beam asymmetry was measured for the first time in $K^0\Sigma^+$ photoproduction. The Bonn–Gatchina PWA, as well as the original and a modified version of K-MAID describe the data fairly well in the intermediate angular range. In the most forward direction the beam asymmetry shows the interesting feature that it turns strongly negative just below the K^* threshold, where a strong decline of the forward cross section was observed [16]. A recent calculation in the chiral unitary framework indicates that this effect may be related to a dynamically generated vector meson–hyperon state [17]. Whether this model is able to reproduce the polarisation data remains to be seen.

Definite conclusions on the reaction mechanism at the prominent structure in the $K^*\Lambda$ and $K^*\Sigma$ threshold region will require the beam asymmetry to be measured across the K^* threshold. In addition, beam-target and beam-recoil double polarisation observables will be necessary to reveal the helicity structure in that energy regime. Such measurements will be subject to future investigations using the CBELSA/TAPS and particularly the new BGO-OD detector setup [40–42] at ELSA.

Acknowledgements

We thank the staff and shift-students of the ELSA accelerator for providing an excellent beam. This work was supported by the federal state of *North-Rhine Westphalia*, the *Deutsche Forschungsgemeinschaft* within the SFB/TR-16 and the *Schweizerischer Nationalfonds*, grant number 200020-132799.

References

[1] L.Ya. Glozman, D.O. Riska, Phys. Rep. 268 (1996) 263.
[2] A. Manohar, H. Georgi, Nucl. Phys. B 234 (1984) 189.
[3] R.H. Dalitz, J.G. McGinley, in: E. Ferrari, G. Violini (Eds.), Low and Intermediate Energy Kaon–Nucleon Physics, Reidel, Boston, 1981, p. 381;
R.H. Dalitz, T.C. Wong, G. Rajasekaran, Phys. Rev. 153 (1967) 1617.
[4] P.B. Siegel, W. Weise, Phys. Rev. C 38 (1988) 2221.
[5] N. Kaiser, T. Waas, W. Weise, Nucl. Phys. A 612 (1997) 297.
[6] C. Garcia-Recio, M.F.M. Lutz, J. Nieves, Phys. Lett. B 582 (2004) 49.
[7] M.F.M. Lutz, E.E. Kolomeitsev, Phys. Lett. B 585 (2004) 243.
[8] B. Borasoy, P.C. Bruns, U.-G. Meißner, R. Nißler, Eur. Phys. J. A 34 (2007) 161.
[9] P.C. Bruns, M. Mai, U.-G. Meißner, Phys. Lett. B 697 (2011) 254.
[10] J.A. Oller, U.-G. Meißner, Phys. Lett. B 500 (2001) 263.
[11] B. Borasoy, U.-G. Meißner, R. Nißler, Phys. Rev. C 74 (2006) 055201.
[12] P. Gonzalez, E. Oset, J. Vijande, Phys. Rev. C 79 (2009) 025209.
[13] S. Sarkar, et al., Eur. Phys. J. A 44 (2010) 431.
[14] E. Oset, A. Ramos, Eur. Phys. J. A 44 (2010) 445.
[15] E. Oset, et al., AIP Conf. Proc. 1388 (2011) 295, arXiv:1103.0807v1 [nucl-th].
[16] R. Ewald, et al., Phys. Lett. B 713 (2012) 180.
[17] A. Ramos, E. Oset, Phys. Lett. B 727 (2013) 287.
[18] R. Ewald, Doctoral Thesis, Bonn 2010.
[19] E. Aker, et al., Nucl. Instrum. Methods A 321 (1992) 69.
[20] R. Novotny, et al., IEEE Trans. Nucl. Sci. 38 (1991) 379.
[21] A.R. Gabler, et al., Nucl. Instrum. Methods A 346 (1994) 168.
[22] W. Hillert, Eur. Phys. J. A 28 (s01) (2006) 139.
[23] D. Elsner, et al., Eur. Phys. J. A 39 (2009) 373.
[24] G. Suft, et al., Nucl. Instrum. Methods A 538 (2005) 416.
[25] E. Gutz, V. Crede, V. Sokhoyan, H. van Pee, et al., Eur. Phys. J. A 50 (2014) 74.
[26] D. Elsner, et al., Eur. Phys. J. A 33 (2007) 147.
[27] G. Knöchlein, D. Drechsel, L. Tiator, Z. Phys. A 352 (1995) 327.
[28] Frank Klein, et al., Phys. Rev. D 78 (2008) 117101.
[29] A.V. Anisovich, et al., Eur. Phys. J. A 47 (2011) 27, and references therein.
[30] D. Drechsel, et al., http://www.kph.uni-mainz.de/MAID/ (Version 29.3.2007).
[31] R. Castelijns, et al., Eur. Phys. J. A 35 (2008) 39.
[32] C.S. Napali, et al., CLAS Collaboration, Phys. Rev. C 87 (2013) 045206.
[33] D. Drechsel, L. Tiator, J. Phys. G 18 (1992) 449.
[34] K. Nakamura, et al., Particle Data Group, J. Phys. G 37 (2010) 075021.
[35] R. Lawall, et al., Eur. Phys. J. A 24 (2005) 275.
[36] W.-T. Chiang, F. Tabakin, Phys. Rev. C 55 (1997) 2054.

[37] A.V. Anisovich, et al., Phys. Lett. B 711 (2012) 162.
[38] L.Ya. Glozman, Phys. Rep. 444 (2007) 1.
[39] E. Klempt, B.C. Metsch, Eur. Phys. J. A 48 (2012) 127.
[40] B. Bantes, et al., Int. J. Mod. Phys. Conf. Ser. 26 (2014) 1460093.
[41] H. Schmieden, Int. J. Mod. Phys. E 19 (2010) 1043.
[42] H. Schmieden, Chin. Phys. C 33 (2009) 1146.